

# A Low-Cost and Robust Maximum Likelihood Doppler Spread Estimator

Fauzi Bellili and Sofiène Affes

INRS-EMT, 800, de la Gauchetière West, Suite 6900, Montreal, Qc, H5A 1K6, Canada.

Emails: {bellili,affes}@emt.inrs.ca

**Abstract**—This paper addresses the problem of Doppler spread estimation in Rayleigh flat fading channels using a new low-cost and robust maximum likelihood (ML) technique. Relying on an elegant approximation of the channel covariance matrix by a two-ray model, we are able to invert the overall approximate covariance matrix analytically thereby obtaining a low-cost closed-form approximation of the likelihood function. We show by computer simulations that the new estimator is accurate over a wide Doppler spread range and that it outperforms many state-of-the-art techniques. In contrast to the latter, it exhibits an unprecedented robustness to the Doppler spectrum shape of the channel since it does not require its *a priori* knowledge.

## I. INTRODUCTION

The environment of mobile communication systems is characterized by a multipath time-varying fading channel where the received signal and its phase are time varying randomly. As known, the fading rate of the channel depends on the Doppler spread (or equivalently the maximum Doppler frequency) which is related to the velocity of the mobile terminal. The Doppler spread is therefore a key parameter for transceiver optimization in mobile communication systems. The characterization of the time variations of such a propagation channel is directly related to the Doppler information. The knowledge of the Doppler parameter or time variations rate (such as the coherence time for example) can be used to optimize the interleaving length in order to reduce the reception delay in addition to optimizing the feedback rate of CSI-based schemes [1]. From the signal processing point of view, the Doppler spread is involved in optimizing the adaptation steps of adaptive channel estimation algorithms [2]. It has also been a key parameter for many other wireless communication applications such as power control and handoff schemes [3-4]. Moreover, due to the very nature of the newly deployed heterogeneous networks (HetNets), the well-known interference mitigation and handoff hysteresis issues are exacerbated when a moving user temporarily enters or even approaches a small cell (i.e., picos or femtos), thereby interfering with its users and possibly resulting in brief macro/small and small/macro cell-reassignments[5]. Reducing interference and avoiding useless handoffs can be achieved by predicting the evolution of the interferer's trajectory through its Doppler spread information (i.e., velocity).

In practice, the Doppler spread estimates are usually obtained from the estimates of the channel coefficients. Then, depending on how the channel estimates are processed, four classes of Doppler estimators are encountered in the open literature: the level-crossing rate (LCR)-based [6-7], the covariance-based [8-10], the spectrum-based [11], and the ML techniques. The

covariance-based estimators are usually preferred as compared to the LCR-based ones. Indeed, the latter need a very large observation window size. Otherwise, the number of crossings may be very small (or there may even be no crossings at all for small Doppler values). The performance of the covariance-based estimators themselves degrades drastically for a relatively small number of received samples, due to a weaker averaging effect (i.e., unreliable estimates of the channel autocorrelation coefficients). The same holds for the spectrum-based ones, since the estimated spectrum is the Fourier transform of these autocorrelation coefficients. In adverse conditions such as in data shortage cases, the ML estimators are known to be the most accurate by relying, among other things, on the direct use of the channel coefficients themselves.

Four ML-based Doppler estimators were previously introduced in the open literature. In fact, one of the first implementations of the ML criterion was proposed in [12] based on the maximization of the power spectral density (PSD) of the estimated channel and a hypothetical one (namely the Jakes' model). Another early ML approach was developed in [13], in the specific context of TDMA transmissions, where periodic pilot symbols are transmitted over each time slot. It involves, however, the numerical inversion of the covariance matrix, a quite demanding operation in complexity. Later, another ML estimator was proposed in [14] using the Whittle approximation. However, it works only for very large normalized Doppler frequencies ( $f_n > 0.1$  where  $f_n = F_d T_s$  and  $T_s$  is the sampling period). Estimation of very low normalized Doppler frequencies is, however, more challenging and more useful. Indeed, current 3G and 4G wireless communication systems and beyond are characterized by high-data-rate transmissions and, hence, require very high sampling rates (e.g., typically  $T_s = 70 \mu s$  in LTE systems [15]). Hence, the target normalized Doppler frequency region for these systems is typically in the range of  $0.0001 \leq f_n \leq 0.03$  for a maximum Doppler frequency  $F_d$  ranging from 1 to 450 Hz. A more recent ML estimator was specifically designed to cope with relatively small normalized Doppler frequencies [16] and, hence, shown to outperform the two previous ML versions<sup>1</sup>. It will be therefore selected as a first benchmark against which we will compare our new ML estimator. In [16], the actual channel autocorrelation function is approximated by a Taylor series of order  $K$  and its complexity remains high as it involves the numerical inversion

<sup>1</sup>Please note that the first ML approach in [12] is also outperformed by a more recent technique introduced in [17], which will be selected as a second benchmark as will be explained shortly below.

of  $(K \times K)$  matrices at each point of the search grid on the top of several matrix multiplications. Another limitation of the four ML estimators [12, 16] discussed above is that they assume the *a priori* knowledge of the channel spectrum form (its analytical expression) and most of them were specifically designed for the very special case of the *uniform* Jakes model.

Motivated by these facts, we develop in this paper a new ML estimator which i) avoids the numerical inversion of the autocorrelation matrix and, therefore, exhibits a very reduced computational complexity; ii) does not require the *a priori* knowledge of the analytical expression of the channel PSD and is robust to its shape; and iii) is able to accurately estimate extremely small normalized Doppler spreads. Indeed, it is based on a second-order Taylor approximation that is valid for most known Doppler PSD models, including the very basic and widely studied *uniform* Jakes the *restricted* Jakes (rJakes) and the Gaussian, biGaussian, rounded, bell, and 3-D flat models, etc. The new estimator is also compared in performance to a more recent technique proposed in [17], selected here as a second benchmark, since it outperforms many other traditional approaches, namely, the HAC technique [10] (which is a combination of [3] and [18]), the ML-based technique in [12], and the Holtzman and Sampath's method [19]. Yet, it will be shown by computer simulations that our new ML estimator outperforms the two selected benchmark techniques, i.e. [16] and [17], over a very wide practical Doppler range, especially in the presence of short data records.

We organize the rest of this paper as follows. In section II, we introduce the system model. In section III, we develop our new ML estimator. In section IV, we assess its performance and compare it to the two selected benchmark techniques as well as the Cramér-Rao lower Bound (CRLB). Finally, we draw out some concluding remarks in section V.

## II. SYSTEM MODEL

Consider an analogous signal,  $x(t)$ , propagating through a flat fading Rayleigh channel,  $h(t)$ , and immersed in an additive noise,  $w(t)$ , which can account also for any interference signal. The baseband received signal can be written as:

$$y(t) = h(t)x(t) + w(t). \quad (1)$$

Observing this baseband analogous signal at pilot positions,  $n_p T_s$ , returns nothing but the estimates of the channel coefficients where  $T_s$  is the sampling period of the system. Likewise, the received signal can be sampled at the rate  $1/T_s$  to provide a set of  $N$  discrete observations  $\{y(nT_s)\}_{n=0}^{N-1}$  from which the channel can be tracked and estimated at both pilot and non-pilot positions,  $nT_s$ . Without loss of generality, we assume that a set of estimates of  $N$  equally-spaced channel coefficients,  $\{\hat{h}(nT_s)\}_{n=0}^{N-1}$ , are made available to the receiver by any channel estimation technique and given by:

$$\hat{h}(nT_s) = h(nT_s) + w(nT_s), \quad n = 0, 1, 2, \dots, N-1, \quad (2)$$

where  $w(nT_s)$  is the estimation error component modelled by a white circular complex Gaussian random variable with mean zero and variance  $\sigma_n^2$ . The statistics of the actual channel coefficients are governed by the unknown Doppler spread to be obtained from the estimates  $\{\hat{h}(nT_s)\}_{n=0}^{N-1}$ . For instance, for the

very specific case of the *uniform* Jakes' model, the channel autocorrelation coefficients,  $r_h(kT_s) = E\{h(nT_s)h((n+k)T_s)^*\}$  where “\*” denotes complex conjugation, are given by:

$$r_h(kT_s) = J_0(\sqrt{2}k\sigma_d T_s) = J_0(2\pi k F_d T_s),$$

where  $J_0(\cdot)$  is the zero-order Bessel function of the first kind and the second equality follows from the relationship between the maximum Doppler frequency and the Doppler spread in the *uniform* Jakes  $\sigma_d = 2\pi F_d/\sqrt{2}$ . In general, this relationship can be explicitly found from the following identity:

$$\sigma_d = \left( \int_{-2\pi F_d}^{2\pi F_d} f^2 S(f) df \right)^{1/2}, \quad (3)$$

where  $S(f)$  is the PSD of the model (i.e., the Fourier transform of the channel autocorrelation coefficients). For instance, for the 3-D scattering model (i.e., flat PSD), the relationship becomes  $\sigma_d = 2\pi F_d/\sqrt{3}$  [17].

As mentioned previously, a distinct advantage of the new ML estimator is its capability of estimating the Doppler spread with almost all known models (cf. Section I) without even knowing its PSD form. For the sake of clarity in the derivations that will follow, it is more convenient to rewrite (2) in a vector form:

$$\hat{\mathbf{h}} = \mathbf{h} + \mathbf{w}, \quad (4)$$

where

$$\begin{aligned} \hat{\mathbf{h}} &= [\hat{h}(0), \hat{h}(T_s), \hat{h}(2T_s), \dots, \hat{h}((N-1)T_s)]^T, \\ \mathbf{h} &= [h(0), h(T_s), h(2T_s), \dots, h((N-1)T_s)]^T, \\ \mathbf{w} &= [w(0), w(T_s), w(2T_s), \dots, w((N-1)T_s)]^T, \end{aligned}$$

We also mention that the expressions “received samples” and “estimated channel coefficients” will be henceforth used interchangeably to refer to the available observations  $\{\hat{h}(nT_s)\}_{n=0}^{N-1}$ .

## III. FORMULATION OF THE NEW ML ESTIMATOR

Owing to (4), it can be shown that  $\hat{\mathbf{h}}$  is a circular symmetric Gaussian random vector whose probability density function, parameterized by the unknown Doppler spread,  $\sigma_d$ , is given by:

$$p(\hat{\mathbf{h}}; \sigma_d) = \frac{1}{\pi^N \det\{\mathbf{R}_{\hat{\mathbf{h}}}(\sigma_d)\}} \exp\left\{-\hat{\mathbf{h}}^H \mathbf{R}_{\hat{\mathbf{h}}}^{-1}(\sigma_d) \hat{\mathbf{h}}\right\}, \quad (5)$$

where  $\mathbf{R}_{\hat{\mathbf{h}}}(\sigma_d)$  is the covariance matrix of the estimated channel,  $\hat{\mathbf{h}}$ , which is given by:

$$\begin{aligned} \mathbf{R}_{\hat{\mathbf{h}}}(\sigma_d) &= E\{\hat{\mathbf{h}}\hat{\mathbf{h}}^H\} \\ &= \mathbf{R}_{\mathbf{h}}(\sigma_d) + \sigma_n^2 \mathbf{I}, \end{aligned} \quad (6)$$

in which  $\mathbf{R}_{\mathbf{h}}(\sigma_d) = E\{\mathbf{h}\mathbf{h}^H\}$  is the the covariance matrix of the *actual* channel. Then, taking the logarithm of (5) and dropping the constant terms yields the log-likelihood function (LLF) as:

$$L(\hat{\mathbf{h}}; \sigma_d) = -\log(\det\{\mathbf{R}_{\hat{\mathbf{h}}}(\sigma_d)\}) - \hat{\mathbf{h}}^H \mathbf{R}_{\hat{\mathbf{h}}}^{-1}(\sigma_d) \hat{\mathbf{h}}. \quad (7)$$

At this early stage, the true challenge of the ML derivation is obvious. Indeed, maximizing  $L(\hat{\mathbf{h}}; \sigma_d)$  with respect to the unknown parameter,  $\sigma_d$ , requires from (7) the inversion of a large-size  $(N \times N)$  covariance matrix and the computation of its determinant. Hence, its computational complexity, in the order

of  $O(N^3)$  operations, increases relatively quite fast with  $N$  (e.g.,  $10^6$  operations at each point of the search grid even for a relatively small  $N = 100$  samples). This suggests that any naive implementation of the ML estimator would be simply too prohibitive in complexity. To avoid the inversion of a large-size covariance matrix, Tsai and Young have recently proposed in [16] an approximate LLF using a  $K$ -order Taylor series expansion that requires the inversion of a  $(K \times K)$  matrix where  $K \ll N$  no matter how large is  $N$  ( $K$  is typically in the range of 10). However, this approximate LLF still requires a series of heavy multiplications of  $(K \times K)$  matrices (on the top of the matrix inversion). Also, the reduced-size approximate matrix being badly conditioned results in numerical instabilities (we will further discuss this limitation later in section IV).

In this paper, we opt for a different approach that avoids any matrix inversion or multiplication, thereby resulting in a very easy and efficient implementation of the ML estimator. To do so, we rely on the following second-order Taylor series approximation of the covariance matrix, developed<sup>2</sup> in [15], which is valid for most known Doppler PSD models (cf. Sections I and II):

$$\mathbf{R}_h(\sigma_d) = \frac{\sigma_h^2}{2} \mathbf{A}(\sigma_d) \mathbf{A}^H(\sigma_d), \quad (8)$$

where

$$\mathbf{A}(\sigma_d) = [\mathbf{a}(-\sigma_d) \quad \mathbf{a}(\sigma_d)], \quad (9)$$

in which  $\mathbf{a}(\sigma)$  is a vector that contains a set of  $N$  uniform samples from a sinusoid of frequency  $\sigma/2\pi$ :

$$\mathbf{a}(\sigma) = [1 \quad e^{j\sigma T_s} \quad e^{j2\sigma T_s} \quad \dots \quad e^{j(N-1)\sigma T_s}]. \quad (10)$$

Now, injecting (8) in (6), an explicit approximate expression for the covariance matrix of the estimated channel is obtained:

$$\mathbf{R}_h(\sigma_d) = \frac{\sigma_h^2}{2} \mathbf{A}(\sigma_d) \mathbf{A}^H(\sigma_d) + \sigma_n^2 \mathbf{I}. \quad (11)$$

As a first step in our quest for finding the analytical inverse of this  $(N \times N)$  matrix and its determinant, we begin by finding the analytical expressions of the non-zero eigenvalues of the matrix  $\mathbf{A}(\sigma_d) \mathbf{A}^H(\sigma_d)$  and their associated eigenvectors. Here, we mention that this matrix is of rank two and thus has two non-zero eigen-values only. Further, it is known from basic linear algebra that the non-zero eigenvalues of  $\mathbf{A}(\sigma_d) \mathbf{A}^H(\sigma_d)$  and  $\mathbf{A}^H(\sigma_d) \mathbf{A}(\sigma_d)$  are the same. Fortunately, the latter matrix is of size  $2 \times 2$  and, thus, its eigen-values can be found analytically. In fact, it can be easily shown that:

$$\mathbf{A}^H(\sigma_d) \mathbf{A}(\sigma_d) = \begin{pmatrix} \|\mathbf{a}(-\sigma_d)\|^2 & \mathbf{a}^H(-\sigma_d) \mathbf{a}(\sigma_d) \\ \mathbf{a}^H(\sigma_d) \mathbf{a}(-\sigma_d) & \|\mathbf{a}(\sigma_d)\|^2 \end{pmatrix}. \quad (12)$$

Then, it can be easily shown that  $\|\mathbf{a}(-\sigma_d)\|^2 = \|\mathbf{a}(\sigma_d)\|^2 = N$  and

$$\begin{aligned} \mathbf{a}^H(-\sigma_d) \mathbf{a}(\sigma_d) &= \sum_{n=0}^{N-1} e^{jn(2\sigma_d T_s)} \\ &= \frac{\sin(N\sigma_d T_s)}{\sin(\sigma_d T_s)} e^{j(N-1)\sigma_d T_s}. \end{aligned} \quad (13)$$

<sup>2</sup>See the details in the Appendix of [17].

Hence, by denoting  $b(\sigma_d T_s) = \frac{\sin(N\sigma_d T_s)}{\sin(\sigma_d T_s)} e^{j(N-1)\sigma_d T_s}$ , the matrix  $\mathbf{A}^H(\sigma_d) \mathbf{A}(\sigma_d)$  is explicitly given by:

$$\mathbf{A}^H(\sigma_d) \mathbf{A}(\sigma_d) = \begin{pmatrix} N & b(\sigma_d T_s) \\ b(\sigma_d T_s)^* & N \end{pmatrix}. \quad (14)$$

After some relatively easy derivations, the two eigenvalues,  $\sigma_1$  and  $\sigma_2$ , of this matrix can be found as:

$$N \pm \left| \frac{\sin(N\sigma_d T_s)}{\sin(\sigma_d T_s)} \right| = N \pm \frac{\sin(N\sigma_d T_s)}{\sin(\sigma_d T_s)}, \quad (15)$$

the second expression in the equation above being dependent on the signum of  $\sin(N\sigma_d T_s)/\sin(\sigma_d T_s)$ . In the sequel, we will assume without loss of generality that  $\frac{\sin(N\sigma_d T_s)}{\sin(\sigma_d T_s)} \geq 0$  and set:

$$\sigma_1 = N + \frac{\sin(N\sigma_d T_s)}{\sin(\sigma_d T_s)} \quad (16)$$

$$\sigma_2 = N - \frac{\sin(N\sigma_d T_s)}{\sin(\sigma_d T_s)} \quad (17)$$

Otherwise, we would just need to swap the definitions of  $\sigma_1$  and  $\sigma_2$ , if  $\frac{\sin(N\sigma_d T_s)}{\sin(\sigma_d T_s)} < 0$ , to always have  $\sigma_1 > \sigma_2$ . And their corresponding eigenvectors would be swapped accordingly thereby resulting in the same decomposition. Then, it can be easily shown that  $[|b(\sigma_d T_s)| \quad b(\sigma_d T_s)^*]^T$  and  $[|b(\sigma_d T_s)| \quad -b(\sigma_d T_s)^*]^T$  are two eigenvectors associated with  $\sigma_1$  and  $\sigma_2$ , respectively, which upon normalization, yield the following two unit-norm eigenvectors:

$$\mathbf{v}_1 = \frac{1}{\sqrt{2}} \begin{bmatrix} 1 & e^{-j(N-1)\sigma_d T_s} \end{bmatrix}^T \quad (18)$$

$$\mathbf{v}_2 = \frac{1}{\sqrt{2}} \begin{bmatrix} 1 & -e^{-j(N-1)\sigma_d T_s} \end{bmatrix}^T. \quad (19)$$

These two eigen-vectors of  $\mathbf{A}^H(\sigma_d) \mathbf{A}(\sigma_d)$  allow us to find the two eigen-vectors,  $\mathbf{u}_1$  and  $\mathbf{u}_2$ , associated to the only non-zero eigen-values  $\sigma_1$  and  $\sigma_2$  of the  $(N \times N)$  approximate covariance matrix of interest  $\mathbf{A}(\sigma_d) \mathbf{A}(\sigma_d)^H$ . In fact, using the singular value decomposition of the matrix  $\mathbf{A}(\sigma_d)$ :

$$\mathbf{A}(\sigma_d) = \mathbf{U} \mathbf{\Sigma}^{1/2} \mathbf{V}^H, \quad (20)$$

where  $\mathbf{V} = [\mathbf{v}_1 \quad \mathbf{v}_2]$ ,  $\mathbf{U} = [\mathbf{u}_1 \quad \mathbf{u}_2]$  and  $\mathbf{\Sigma} = \text{diag}(\sigma_1, \sigma_2)$ , it can be shown from (20) that the matrix  $\mathbf{U}$  of interest is obtained as:

$$\mathbf{U} = \mathbf{A}(\sigma_d) \mathbf{V} \mathbf{\Sigma}^{-1/2}. \quad (21)$$

Hence,  $\mathbf{u}_1$  and  $\mathbf{u}_2$  are given by:

$$\mathbf{u}_1 = \frac{1}{\sqrt{\sigma_1}} \mathbf{A}(\sigma_d) \mathbf{v}_1, \quad (22)$$

$$\mathbf{u}_2 = \frac{1}{\sqrt{\sigma_2}} \mathbf{A}(\sigma_d) \mathbf{v}_2. \quad (23)$$

Now, we define the matrix  $\mathbf{J}$  as:

$$\mathbf{J} = \begin{pmatrix} 0 & \dots & \dots & 0 & 1 \\ \vdots & & \ddots & 1 & 0 \\ \vdots & \ddots & \ddots & \ddots & \vdots \\ 0 & 1 & \ddots & & \vdots \\ 1 & 0 & \dots & \dots & 0 \end{pmatrix}. \quad (24)$$

and note that:

$$e^{-j(N-1)\sigma_d T_s} \mathbf{a}(\sigma_d) = \mathbf{J} \mathbf{a}(-\sigma_d). \quad (25)$$

Therefore, taking into account (9), (18) and (22), we obtain:

$$\begin{aligned} \mathbf{u}_1 &= \frac{1}{\sqrt{2\sigma_1}} \left( \mathbf{a}(-\sigma_d) + e^{-j(N-1)\sigma_d T_s} \mathbf{a}(\sigma_d) \right) \\ &= \frac{1}{\sqrt{2\sigma_1}} (\mathbf{I} + \mathbf{J}) \mathbf{a}(-\sigma_d). \end{aligned} \quad (26)$$

Likewise,  $\mathbf{u}_2$  is given by:

$$\begin{aligned} \mathbf{u}_2 &= \frac{1}{\sqrt{2\sigma_2}} \left( \mathbf{a}(-\sigma_d) - e^{-j(N-1)\sigma_d T_s} \mathbf{a}(\sigma_d) \right) \\ &= \frac{1}{\sqrt{2\sigma_2}} (\mathbf{I} - \mathbf{J}) \mathbf{a}(-\sigma_d) \end{aligned} \quad (27)$$

After some algebraic manipulations, it can be shown that the vectors  $\mathbf{u}_1$  and  $\mathbf{u}_2$  are given by  $\mathbf{u}_1 = \frac{\sqrt{2}}{\sqrt{\sigma_1}} e^{-j\frac{N-1}{2}\sigma_d T_s} \tilde{\mathbf{u}}_1$  and  $\mathbf{u}_2 = j \frac{\sqrt{2}}{\sqrt{\sigma_2}} e^{-j\frac{N-1}{2}\sigma_d T_s} \tilde{\mathbf{u}}_2$  where :

$$\tilde{\mathbf{u}}_1 = \begin{bmatrix} \cos\left(\frac{N-1}{2}\sigma_d T_s\right) \\ \cos\left(\frac{N-3}{2}\sigma_d T_s\right) \\ \vdots \\ \cos\left(\frac{N-2k}{2}\sigma_d T_s\right) \\ \vdots \\ \cos\left(\frac{N-2k}{2}\sigma_d T_s\right) \\ \vdots \\ \cos\left(\frac{N-2k}{2}\sigma_d T_s\right) \\ \vdots \\ \cos\left(\frac{N-3}{2}\sigma_d T_s\right) \\ \cos\left(\frac{N-1}{2}\sigma_d T_s\right) \end{bmatrix} \quad \tilde{\mathbf{u}}_2 = \begin{bmatrix} \sin\left(\frac{N-1}{2}\sigma_d T_s\right) \\ \sin\left(\frac{N-3}{2}\sigma_d T_s\right) \\ \vdots \\ \sin\left(\frac{N-2k}{2}\sigma_d T_s\right) \\ \vdots \\ \vdots \\ -\sin\left(\frac{N-2k}{2}\sigma_d T_s\right) \\ \vdots \\ -\sin\left(\frac{N-3}{2}\sigma_d T_s\right) \\ -\sin\left(\frac{N-1}{2}\sigma_d T_s\right) \end{bmatrix}. \quad (28)$$

Then, from (20), we obtain:

$$\mathbf{A}(\sigma_d) \mathbf{A}(\sigma_d)^H = \mathbf{U} \mathbf{\Sigma} \mathbf{U}^H \quad (29)$$

Therefore, from (11), the approximate covariance matrix of the received samples (or estimated channel coefficients) is given by:

$$\mathbf{R}_{\hat{\mathbf{h}}}(\sigma_d) = \frac{\sigma_h^2}{2} \mathbf{U} \mathbf{\Sigma} \mathbf{U}^H + \sigma_n^2 \mathbf{I}. \quad (30)$$

Now using the Woodbury identity, it can be shown that:

$$\mathbf{R}_{\hat{\mathbf{h}}}^{-1}(\sigma_d) = \frac{1}{\sigma_n^2} \mathbf{I} - \frac{1}{\sigma_n^2} \mathbf{U} \left( \frac{2}{\rho} \mathbf{\Sigma}^{-1} + \mathbf{U}^H \mathbf{U} \right)^{-1} \mathbf{U}^H, \quad (31)$$

where  $\rho = \frac{\sigma_h^2}{\sigma_n^2}$  is the SNR of the received signal (or channel estimate). The unit-norm vectors  $\mathbf{u}_1$  and  $\mathbf{u}_2$  are orthogonal as can be seen from (28) and thus  $\mathbf{U}^H \mathbf{U} = \mathbf{I}$ . Consequently, the matrix  $\frac{2}{\rho} \mathbf{\Sigma}^{-1} + \mathbf{U}^H \mathbf{U}$  is in fact diagonal and its inverse is easily obtained by inverting its diagonal elements. After some algebraic manipulations, we obtain:

$$\mathbf{R}_{\hat{\mathbf{h}}}^{-1}(\sigma_d) = \frac{1}{\sigma_n^2} \mathbf{I} - \frac{1}{\sigma_n^2} \mathbf{U} \mathbf{\Sigma}_\rho \mathbf{U}^H, \quad (32)$$

where  $\mathbf{\Sigma}_\rho = \text{diag} \left( \frac{\rho\sigma_1}{2+\rho\sigma_1}, \frac{\rho\sigma_2}{2+\rho\sigma_2} \right)$ . The determinant of  $\mathbf{R}_{\hat{\mathbf{h}}}$  is also analytically obtained as the product of its eigenvalues as follows:

$$\det \{ \mathbf{R}_{\hat{\mathbf{h}}} \} = \frac{\sigma_n^{2N}}{4} (2 + \rho\sigma_1) (2 + \rho\sigma_2). \quad (33)$$

Finally, substituting (32) and (33) into (7) and dropping the constant terms (that do not depend on the unknown Doppler spread), the LLF of the system reduces simply to:

$$L(\hat{\mathbf{h}}; \sigma_d) = \log \left( (2 + \rho\sigma_1)(2 + \rho\sigma_2) \right) + \frac{1}{\sigma_n^2} \left\| \mathbf{\Sigma}_\rho^{1/2} \mathbf{U}^H \hat{\mathbf{h}} \right\|^2, \quad (34)$$

This approximate likelihood expression involves the noise variance,  $\sigma_n^2$ , and the SNR,  $\rho$ , which are also unknown in practice. In this work, they are estimate as follows. We form a  $(p \times p)$  Toeplitz matrix from the first  $p$  estimated correlation coefficients where  $p = 20$ . Owing to the two-ray approximation model in (8), this matrix is also of rank 2. Therefore, its 10 (actually  $p - 2$ ) smallest eigenvalues are nothing but multiple estimates of the unknown noise variance which can be averaged together to obtain a more refined estimate,  $\hat{\sigma}_n^2$ , of  $\sigma_n^2$ . Further, the zero-lag estimated correlation coefficient is given by  $\hat{r}_{\hat{\mathbf{h}}}(0) = \sigma_h^2 + \sigma_n^2$ , from which the channel power is obtained as  $\hat{\sigma}_h^2 = \hat{r}_{\hat{\mathbf{h}}}(0) - \hat{\sigma}_n^2$ . The SNR estimate is then obtained as  $\hat{\rho} = \hat{\sigma}_h^2 / \hat{\sigma}_n^2$ . Then, by injecting these estimates in (34) and expanding the norm term, the LLF becomes:

$$\begin{aligned} L(\hat{\mathbf{h}}; \sigma_d) &= \log \left( (2 + \hat{\rho}\sigma_1)(2 + \hat{\rho}\sigma_2) \right) + \\ &\quad \frac{1}{\hat{\sigma}_n^2} \sum_{i=1}^2 \sqrt{\frac{\hat{\rho}\sigma_i}{2 + \hat{\rho}\sigma_i}} \left| \mathbf{u}_i^H \hat{\mathbf{h}} \right|^2. \end{aligned} \quad (35)$$

Then ML estimate,  $\hat{\sigma}_d$ , of the Doppler spread is given by:

$$\hat{\sigma}_d = \arg \max_{\sigma_d} L(\hat{\mathbf{h}}; \sigma_d) \quad (36)$$

It can be easily obtained numerically with a very light grid search. In fact, as highlighted by (35), the LLF breaks down into the sum of two inner-product terms which can be rapidly evaluated at each point  $\sigma_d$  of the grid<sup>3</sup>, and hence the new estimator is of very low computational cost. This is in contrast to the recent ML implementation introduced in [16] where, at each grid point, it involves the numerical inversion of a  $(K \times K)$  approximation matrix and  $K$  multiplications of other predefined matrices of the same size. Moreover, in contrast to the simple LLF of (35) which is valid for most common Doppler PSD models (cf. Sections I and II), the ML implementation in [16] relies on a different Taylor series expansion for each model and, hence, requires its unpractical knowledge *a priori*.

#### IV. SIMULATION RESULTS

In this section, we assess the new ML estimator using the normalized mean square error (NMSE) as a performance metric. The NMSE is computed using 2000 Monte-Carlo runs. The two recent techniques selected as benchmarks, i.e., [16] and [17] (cf. Section I), outperform many other state-of-the-art approaches (see references therein). The estimator proposed in [17] is based on a covariance matching technique and hence it is referred to here as COMAT. The estimator proposed in [16] is referred to here as TAML for time-domain approximate ML. For illustration purposes, we consider the case of the *uniform* Jakes model. Note that although COMAT was developed as the first estimator to be

<sup>3</sup>The procedure of estimating the noise variance and the SNR is performed only once before the grid-search task.

oblivious in its derivations to the Doppler PSD model, it requires in its implementation an appropriate selection of the correlation lags that could be sensitive to noticeable PSD model mismatches.

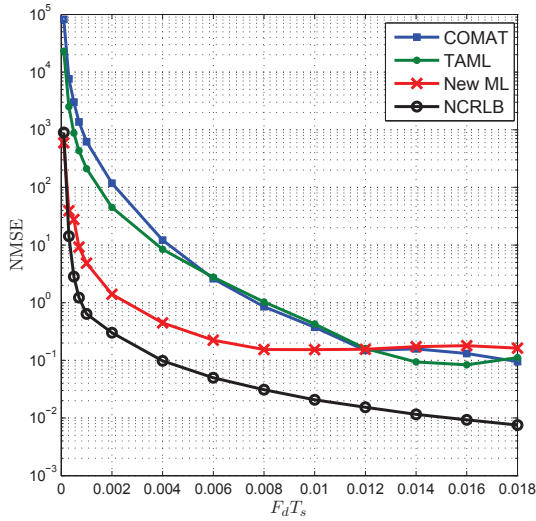


Fig. 1. NMSE of the three estimators vs.  $F_d T_s$  at  $T_s = 10 \mu\text{s}$ , an SNR = 0 dB, and  $N = 100$ .

Fig. 1 shows the performance of the three estimators for an observation window size of  $N = 100$  samples. The new ML estimator outperforms the two benchmark techniques over a wide range of the normalized Doppler frequency  $f_n = F_d T_s$ , i.e., over  $0.0001 \leq f_n \leq 0.012$ . On one hand, COMAT is covariance-based and therefore suffers from a weaker averaging effect at relatively small values of  $N$ . On the other hand, TAML suffers from numerical instabilities due to the numerical inversion of badly conditioned matrices. This can be observed very clearly from the plot of different realizations of its approximate LLF in Fig. 2(a) for a true Doppler frequency  $F_d = 1000$  Hz. In this figure, we see that the TAML's LLF exhibits a true maximum near  $F_d = 1000$  Hz, but it is dominated by another spurious maximum located approximately at  $F_D = 2300$  Hz stemming from numerical instabilities. This is in contrast to the new ML estimator's LLF in Fig. 2(b), which is always smooth and exhibits a single maximum relatively near the true Doppler frequency value  $F_d = 1000$  Hz.

Such wrong maxima make TAML extremely biased, as can be seen from Fig. 3. This figure shows, however, that the new ML exhibits a reduced bias. Therefore, when a larger number of data records is available, there is room, as far as the new ML estimator is concerned, for averaging over local windows of size  $M = 100$  so as to enhance the estimation accuracy. This is depicted in Fig. 4 where we plot the NMSE of the three estimators using  $N = 1000$  received samples. In this figure, the new ML approach estimates the Doppler frequency over each block of  $M = 100$  samples and then averages all the  $N/M$  individual estimates as a final refined estimate. The COMAT estimator is applied using the entire block of received samples and, hence, its performance improves remarkably. This is due to the fact that the correlation coefficients are quite accurately estimated in the presence of a large number of received samples.

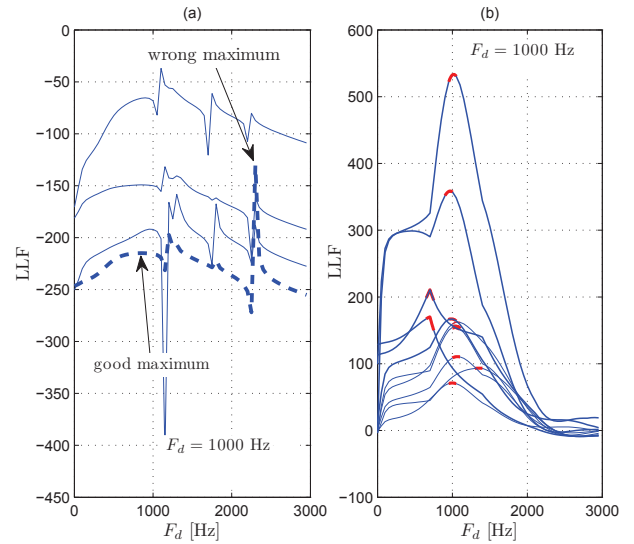


Fig. 2. LLFs vs.  $F_d$  for a true  $F_d = 1000$  Hz at an SNR = 0 dB: (a) TAML, (b) New ML.

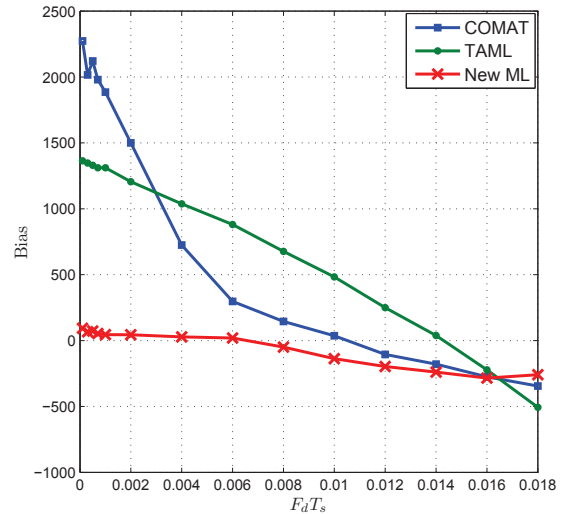


Fig. 3. Estimation bias of the three estimators vs.  $F_d T_s$  at  $T_s = 10 \mu\text{s}$ , an SNR = 0 dB, and  $N = 100$ .

Yet, the new ML estimator exhibits the best performance over the entire Doppler range (except for a minor advantage for TAML in the very high Doppler range). But taking into account their performance/complexity tradeoffs and their dependence on or obliviousness to the knowledge of the PSD shape, the new ML approach is more cost-effective and robust as well. Finally in Fig. 5, we plot the NMSE of both COMAT and the new ML estimator for a 3-D flat PSD model. TAML is not plotted here since it is mainly derived for the uniform Jakes. It is seen that the new ML outperforms COMAT over a wide range of normalized Doppler spreads. This stems from the increased robustness of the new ML estimator to the Doppler type since it applies directly to the received samples without the need for an appropriate choice of the correlation lags as required by COMAT (cf. above).

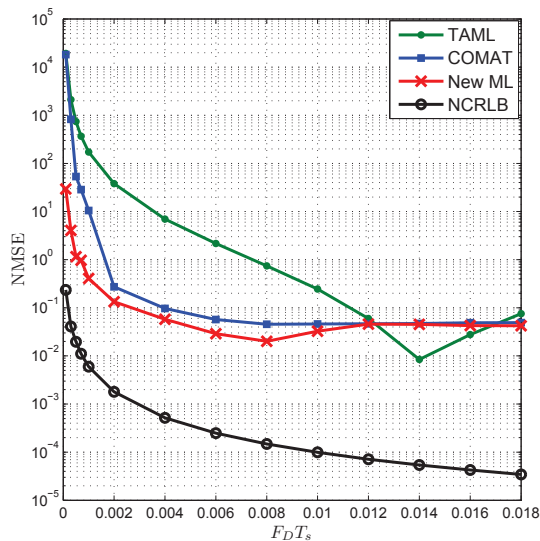


Fig. 4. NMSE of the three estimators vs.  $F_D T_s$  at  $T_s = 10 \mu s$ , an SNR = 0 dB, and  $N = 1000$ .

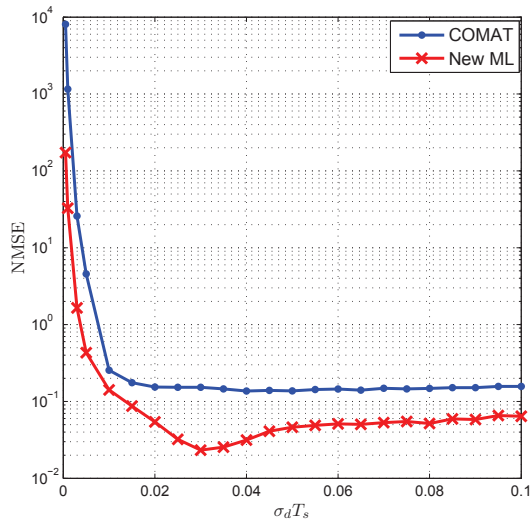


Fig. 5. NMSE of COMAT and the new ML estimator vs.  $\sigma_d T_s$  at  $T_s = 10 \mu s$ , an SNR = 0 dB, and  $N = 1000$ .

## V. CONCLUSION

In this paper, we derived a new ML estimator for the Doppler spread geared toward current and next generations of high-data-rate wireless communication systems. Indeed, it is able to accurately estimate extremely low normalized Doppler frequencies that are typical of these new systems. It is applicable to most used Doppler types without knowledge of their PSD shape. In contrast to all previous ML implementations, the new estimator does not involve any numerical matrix inversion and therefore requires a relatively very low computational cost. It also outperforms the state-of-the-art estimators over a wide range of the normalized Doppler spread, more so at the very useful low values region that is typical of current and next generations of high-data-rate wireless communication systems.

## REFERENCES

- [1] D. N. C. Tse and P. Viswanath, *Fundamentals of Wireless Communications*, Cambridge Univ. Press, 2005.
- [2] S. Affes and P. Mermelstein, "A new receiver structure for ssynchronous CDMA: STAR-the spatio-temporal array-receiver", *IEEE Jour. Selected Areas in Commun.*, vol. 16, no. 8, pp. 1411-1422, Oct. 1998.
- [3] C. Tepedelenioglu, A. Abdi, G. B. Giannakis, and M. Kaveh, "Estimation of Doppler spread and signal strength in mobile communications with applications to handoff and adaptive transmission," *Wireless Communications and Mobile Computing*, vol. 1, pp. 221-242, 2001.
- [4] G. L. Stüber, *Principles of Mobile Communication*, 2nd ed., Kluwer, 2001.
- [5] S. K. Lee, K. Sriram, K. Kim, Y. H. Kim, and N. Golmie, "Vertical handoff decision algorithms for providing optimized performance in heterogeneous wireless networks," *IEEE Trans. Veh. Technol.*, vol. 58, no. 2, pp. 865-881, Feb. 2009.
- [6] M. D. Ausint and G. L. Stuber "Velocity adaptive handoff algorithms for microcellular systems," *IEEE Trans. Veh. Technol.*, vol. 43, no. 3, pp. 549-561, Aug. 1994.
- [7] G. Park, D. Hong and C. Kang "Level crossing rate estimation with Doppler adaptive noise suppression technique in frequency domain," in *Proc. IEEE VTC'2003-Fall*, pp. 1192-1195, 2003.
- [8] K. Baddour and N. C. Beaulieu "Robust Doppler spread estimation in nonisotropic fading channels", *IEEE Trans. Wireless Commun.*, vol. 4, no. 6, pp. 2677-2682, Nov. 2005.
- [9] C. Tepedelenioglu and G. B. Giannakis "On velocity estimation and correlation properties of narrowband mobile communication channels," *IEEE Trans. Veh. Technol.*, vol. 50, no. 4, pp. 1039-1052, July 2001.
- [10] O. Mauritz "A hybrid method for Doppler spread estimation," in *Proc. IEEE VTC'2004-Spring*, pp. 962-965, 2004.
- [11] S. Mohanty, "VEPSD: Velocity estimation using the PSD of the received signal envelope in next generation wireless systems," *IEEE Trans. Wireless Comm.*, vol. 4, no. 6, pp. 2655-2660, Nov. 2005.
- [12] H. Hansen, S. Affes, and P. Mermelstein, "A Rayleigh Doppler frequency estimator derived from maximum likelihood theory," in *Proc. IEEE SPAWC'1999*, pp. 382-386, 1999.
- [13] L. Krasny, H. Arslan, D. Koilpillai, and S. Chennakeshu, "Doppler spread estimation in mobile radio systems," *IEEE Commun. Lett.*, vol. 5, no. 5, pp. 197-199, May 2001.
- [14] A. Dogandi and B. Zhang, "Estimating Jakes Doppler power spectrum parameters using the whittle approximation," *IEEE Trans. Signal Process.*, vol. 53, no. 3, pp. 987-1005, Mar. 2005.
- [15] 3GPP TS 36.211: 3rd Generation Partnership Project; Technical Specification Group Radio Access Network; Evolved Universal Terrestrial Radio Access (E-UTRA); Physical Channels and Modulation.
- [16] Y.-R. Tsai and K.-J. Yang, "Approximate ML Doppler spread estimation over flat Rayleigh fading channels," *IEEE Signal. Process. Lett.*, vol. 16, no. 11, pp. 1007-1010, Nov. 2009.
- [17] M. Souden, S. Affes, J. Benesty and R. Bahroun "Robust Doppler spread estimation in the presence of a residual carrier frequency offset," *IEEE Trans. Signal Process.*, vol. 57, no. 10, pp. 4148-4153, Oct. 2009.
- [18] D. Sandberg, "Method and apparatus for estimating Doppler spread," U.S. Patent 6922452, application no. 09/812956, Mar. 27, 2001, prior publication data: US 2002/0172307 A1 Nov. 21, 2002, issued on July 26, 2005.
- [19] J. Holtzman and A. Sampath, "Adaptive averaging methodology for handoffs in cellular systems," *IEEE Trans. Veh. Technol.*, vol. 44, no. 1, pp. 59-66, Feb. 1995.